L-Cysteine Interaction with Au-55 Nanoparticle

ARTICLE *in* THE JOURNAL OF PHYSICAL CHEMISTRY C · DECEMBER 2012

Impact Factor: 4.77 · DOI: 10.1021/jp308215n

5 AUTHORS, INCLUDING:

Jessica Ann Carr
Massachusetts Institute of Technology
4 PUBLICATIONS **21** CITATIONS
SEE PROFILE

Hong Wang
West Virginia University
24 PUBLICATIONS **732** CITATIONS
SEE PROFILE

James P Lewis
West Virginia University
90 PUBLICATIONS **2,790** CITATIONS
SEE PROFILE

THE JOURNAL OF PHYSICAL CHEMISTRY C

Article

pubs.acs.org/JPCC

L-Cysteine Interaction with Au_{55} Nanoparticle

Jessica A Carr,[‡] Hong Wang,*[,†] Anuji Abraham,[‡] Terry Gullion,[‡] and James P. Lewis[†]

[†]Department of Physics, West Virginia University, Morgantown, West Virginia 26506-6315, United States

[‡]Department of Chemistry, West Virginia University, Morgantown, West Virginia 26506-6315, United States

Supporting Information

ABSTRACT: Simulations of L-cysteine molecules attaching on Au nanoparticles provide insight on how larger biomolecules (such as proteins and peptides) can interact with Au nanoparticles. The attaching mode is still in debate and of strong impact on the fundamental research in biosensors and biomedicine. We used a density functional theory (DFT) approach to calculate the interactions between L-cysteine molecules and the quantum sized Au nanoparticle Au_{55}. Our results support the attaching mode recognized in solid-state NMR studies, which indicate that a double layer of L-cysteine molecules is the likely configuration. A strong electronic interaction between gold and sulfur atoms establishes a strong-bonding inner layer, while a hydrogen-bond network between zwitterion-structured cysteine molecules stabilizes the existence of a second layer with thiol (−SH) groups oriented outward. Such a structure has high potential for further biofunctionalization.

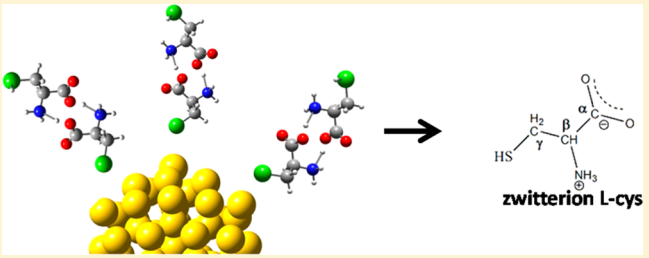

1. INTRODUCTION

The chemistry of gold (Au) nanoparticles has recently attracted extensive research interests and practical attention due to the versatility of their application in the field of nanotechnology, self-assembly, catalysis, and molecular electronics.[1−5] In particular, the promising properties exhibited by biofunctionalized Au nanoparticles have driven intense interests both in biomedical and bioanalytical areas, such as controlled drug delivery, medical diagnosis, and biosensors.[4,6,7] Therefore, understanding the fundamental mechanisms and properties of biofunctionalized Au nanoparticles is becoming critical for current organic−inorganic nanosystems design and development in the related application areas.

In general, amino acids are considered suitable agents in the biofunctionalization of gold nanoparticles due to the presence of different functional groups such as −SH or $-NH_2$, which are able to bond to the gold nanoparticle surface.[8−11] Cysteine is the only amino acid having a thiol group, an amino group, and a carboxyl group, which create several possibilities for bonding to the metal surface.[11−14] In addition, under certain environmental conditions, cysteine can exist as a zwitterion structure in which the amino and carboxyl groups have an induced charge (they become $-NH_3^+$ and $-COO^-$).[15] Understanding how these functional groups interact with the gold nanoparticle surface is important to further the investigation in biofunctionalization of the gold particle with either peptides or proteins. Among the three functional groups (−SH, $-NH_2$, and −COOH), thiol groups have been studied extensively due to the strong bonding features exhibited in thiol−gold systems. A recent study regarding the thiol ligand protected gold nanoparticle (Au_{102}) shows that the thiol ligands (*p*-MBA in this study) coverage around the gold nanoparticle is much higher compared to the coverage on gold surfaces, which is accounted for the curvature of the gold nanoparticle appearance.[16] Jadzinsky et al. proposed a staple motif containing alternative gold and sulfur atoms along the surface curvature. This motif represents a stable intermediate for forming larger nanoparticles during the chemical synthesis process. A subsequent DFT study[17] adopted Au_{38} nanocluster as a theoretical model and establishes the staple motif for Au nanoparticles with high thiol ligand coverage. Other relevant studies also show that the steric effect between thiold ligands plays an important role in determining the coverage as well.[18,19] Therefore, not only the bonding feature of Au−S bonds but also the steric effect existing between ligands both play an important role in the interaction between the ligands and gold nanoparticles.

So far, the main studies regarding the cysteine attaching mode focus on cysteine adsorption on Au(111) or (110) surfaces.[20−22] An STM study combined with DFT calculations investigated the chiral adsorption of cysteine monolayers on the Au(110) surface and proposed a conceptual three-point contact model, which suggests that cysteine most likely employs multiple functional groups in its bonding to gold surfaces.[21] Several other DFT studies have focused primarily on the sulfur binding at the bridge and fcc hollow sites and the associated molecular conformations.[20,23,24]

Even though extensive effort has been revived to identify a clear perspective of the cysteine attaching mode on a metal surface, it appears that organic−metal coupling may vary substantially and exhibit different configurations. In particular,

Received: August 17, 2012
Revised: October 31, 2012
Published: November 21, 2012

cysteine does not exist as an isolated molecule; thus, for practical biofunctionalization of the gold particle surface, the organic−metal coupling and the intermolecular forces between cysteine molecules both need to be considered in cysteine−metal systems. Besides, gold nanoparticles are fundamentally different from gold surfaces. For example, the surface to volume ratio and the shape are both important factors that distinguish gold nanoparticles from gold surface structures. Recent solid-state NMR studies proposed a bilayer cysteine boundary around gold nanoparticles as opposed to the single layer observed for gold surfaces.[14,25] The NMR work suggests that the first layer is made of cysteine molecules forming S−Au bonds with the gold surface and has charged amino and carboxylate groups oriented outward. The outer layer interacts with the inner layer through hydrogen-bond intermolecular forces and has the thiol groups pointing outward, which make it possible to bond other biomolecules for desired biofunctionalization of gold nanoparticles.

In our study, we primarily focus on investigating how cysteine molecules attach on quantum sized gold nanoparticles using DFT calculations. One question is how multiple cysteine molecules arrange around the Au nanoparticle. We aim to determine whether the monolayer model or the bilayer model of cysteine molecules arranging around the gold nanoparticle is preferred and if the zwitterion is the favored structural format of cysteine in this complex system. We optimize the geometry of several possible configurations and analyze the charge transfer occurring in the cysteine−gold complex at an atomic level. We also calculate the adsorption energy associated with each structure and focus on those models with the strongest interaction between gold and cysteine molecules.

2. COMPUTATIONAL METHODS

We carried out density functional theory (DFT) calculations using the DMol3 module implemented in Materials Studio 5.5.[26,27] Geometric optimizations of $Au_{55}[cysteine]_n$ and the Au_{55} nanoparticle itself were performed by using local density approximation (LDA) with the Perdew−Wang (PWC) functional. Polarization was included in the double numerical basis set (DNP and DND) while considering only effective core potentials (ECP) in all calculations involving cysteine on Au_{55}. Otherwise, all-electrons were considered in the optimization of the cysteine molecule by itself. The self-consistent-field calculation had convergence criteria of 10^{-5} Hartree and the tolerances of energy, maximum force, and maximum displacement for the geometry optimization were set to be 1.0×10^{-4} au, 0.02 au, and 0.05 au, respectively.

By way of comparison, we calculated the single-point energy of the optimized structures using generalized gradient approximation (GGA)[28] in the form of Perdew−Burke−Ernzerhof (PBE) functional, which has been used in many previous DFT studies of gold nanoparticles with ligand molecules attached. The d-polarization was included in the double numerical basis set (DND) with the effective core potential (ECP) again chosen in all the calculations regarding the Au_{55} with cysteine attaching. All other parameters were chosen to be the same as in the LDA calculations. In addition to the DFT calculations in this study, we included the dispersion energy calculations by using the DFT-D3 package.[29−33] DFT-D3 is an atom-pair wise dispersion correction, which enables to add dispersion energy to the KS-DFT energies:

$$E_{DFT-D3} = E_{KS-DFT} - E_{disp}$$

with E_{disp} being the sum of the two- and three-body contributions to the dispersion energy. Using the DFT-D3 package, we compute the dispersive energy with the optimized coordinated achieved via Dmol3 calculation. The dispersion energies of all the configurations studied in this work are listed in the Supporting Information.

For the initial atomic structure of the cysteine molecule, we removed a single molecule from the solid L-cysteine crystal structure. In solid-state L-cysteine, each cysteine molecule is in the zwitterion configuration with charged amino and carboxylate groups, which are stabilized by an intermolecular H-bond network existing between all the cysteine zwitterions.[34,35] We selected the zwitterion cysteine because the charged functional groups of the zwitterion structure could potentially interact with neighboring adsorbates through hydrogen bonds; therefore, facilitating future biofunctionalization. However, the optimized structure of the cysteine molecule shows that one of the three H atoms in the charged amino group moves back to the carboxylate group due to a desire for maintaining a neutral structure, shown in Figure 1. Then, we

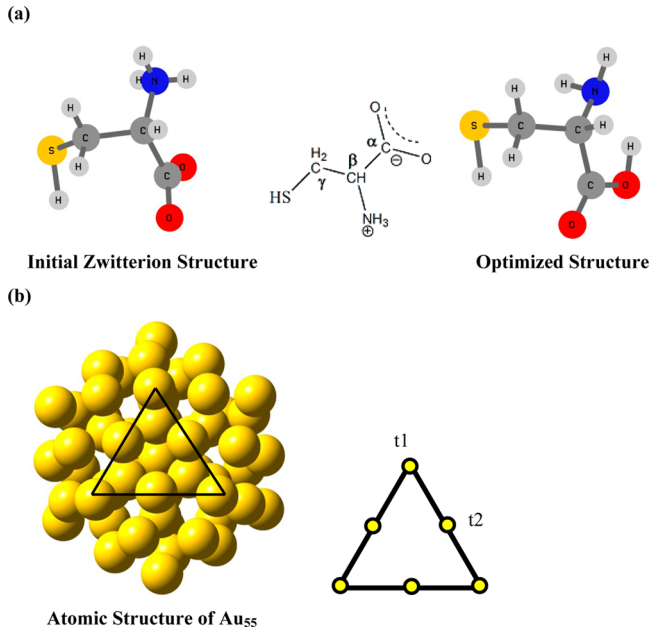

Figure 1. (a) Atomic structures of cysteine zwitterions and neutral cysteine. (b) Icosahedral structure of Au_{55} with the triangle labeled as the fcc-structural character.

considered three attaching modes for this cysteine structure on Au_{55}: via −SH, $-NH_2$, and −COOH. Previous work showed that cysteine can attach to the gold surface via both the amino and the thiol side group.[36,37] As for the carboxyl group, experimental studies have shown that, in cysteine molecules, they are engaged in intermolecular bonds and do not bind to the metal surface.[38] However, since we are using Au_{55} nanoclusters to model the gold nanoparticle, we still consider −COOH as one possible attaching mode.

The 55-atom gold nanocluster was chosen as the model in this study, as it has been studied extensively both in experimental and computational fields.[39−41] Au_{55} indicates unique cytotoxicity, which seems to be caused by the unusually strong interaction between the 1.4 nm particles and the major

dx.doi.org/10.1021/jp308215n | J. Phys. Chem. C 2012, 116, 25816−25823

grooves of DNA.[42] The atomic structure of Au_{55} used in this study is the icosahedral structure, which is accepted as the most stable geometry of the well-known high symmetry arrangements such as icosahedral, cuboctahedral, and decahedral structures.[43] This structure is shown in Figure 1. The size of Au_{55} is around 1.4 nm, which is a moderate size for DFT approach to deliver reliable data for a practical comparison with experimental studies. It should be noted that there are 20 equivalent triangular fcc (111)-like faces in the Au_{55} structure, labeled in Figure 1 as well. Thus, we considered two nonequivalent sites t1 and t2 for each attaching mode.

3. RESULTS AND DISCUSSION

Even though some DFT studies have demonstrated that cysteine molecules attach on gold surface via two possible modes, either by the −SH group or the $-NH_2$ group, the attaching preference appears different for gold nanoparticles since they are fundamentally different from gold surfaces. Thus, we considered three possible attaching modes at each of the two attaching sites (t1 and t2) (shown in Figure 1) in our initial study of a single cysteine molecule's interaction with the nanoparticle. It turns out that the −SH attaching mode at t1, which corresponds to an Au−S covalent bond, has the lower adsorption energy (−0.490 eV, shown in S1 of Supporting Information) compared to the other two attaching modes (the adsorption energies are positive for $-NH_2$ and −COOH mode) at the t1 site. The total energies of all the optimized structures are listed in Table 1. For the t2 sites, even though the total energy of −SH mode is slightly lower than that of the −SH mode on t1, the bond distance between the functional groups and the attached gold atoms are much longer than the bond distance 2.36 Å of the former case. For example, the distance between O (−COOH) and the Au (t2) atom is about 2.48 Å, which indicates that the interaction between −COO and Au is weaker than that between Au−S, which is consistent with the bond strength proposed in the previous study.[44] Therefore, combining these two factors together, we propose that −SH is more favorable for a single cysteine molecule attaching on Au_{55} than the other two groups ($-NH_2$) and (−COOH). The following confirmations are the derivative of the −SH attaching mode either at the t1 or t2 sites.

Table 1. Total Energy of Adsorption Modes via Different Functional Groups, −SH, $-NH_2$, and −COOH, and via the Nonequivalent Sites of the Triangular Au_{55} Nanoparticles Surface, t1 and t2; the Bond Distance between the Attaching Atom and the Gold Atom

complex	total energy (a.u)	bond distance
t1		
Au_{55} + cysteine(SH)	−8191.475	Au−S 2.36 Å
Au_{55} + cysteine(NH_2)	−8191.426	Au−N 2.10 Å
Au_{55} + cysteine(COOH)	−8191.436	Au−C 2.24 Å
t2		
Au_{55} + cysteine(SH)	−8191.480	Au−S 2.42 Å
Au_{55} + cysteine(NH_2)	−8191.420	Au−N 2.38 Å
Au_{55} + cysteine(COOH)	−8191.450	Au−C 2.48 Å

3.1. Multicysteine Molecules Attaching Model. On the basis of the −SH attaching mode, we extended the investigation to the attaching mode of multiple cysteine molecules adsorbing on Au_{55}. One question is how multiple cysteine molecules arrange around the nanoparticle. In general, it is established that L-cysteine is able to stabilize the gold nanoparticles and assemble into supermolecules.[3] The monolayer model is extensively accepted for cysteine molecules wrapping around gold nanoparticles. In our study, to determine the attaching mode of multiple cysteine molecules at an atomic level, we systematically selected a numbers of cysteine molecules and divided them into two groups. One group contained all the cysteine molecules attaching on Au_{55} via thiol groups and forming a monolayer complex, shown in Figure 2. In this model, the cysteine molecules disperse around the gold nanoparticle surface, and the initial intermolecular H-bond network in solid L-cysteine is broken spontaneously. In the second group, the cysteine molecules attach on Au_{55} nanoparticle via pairs. One cysteine molecule of the pair attaches to Au_{55} via a thiol group, while the outer cysteine molecule interacts with the inner cysteine by $-NH_2\cdots$COOH and $-$COOH$\cdots NH_2$ intermolecular H-bonding interactions, similar to the H-bond network in solid L-cysteine. These models are shown in Figure 3. It should be pointed out that the process of the adsorption of thiols on different metal surfaces has been studied and considered a complex reaction pathway, comprised by a few steps differing in time scale.[45] During the course of the adsorption process, the rate limiting step is the cleavage of the H−S bond, which can be alternatively explained in a homolytic fashion to form a RS-Au bond and the hydrogen atoms to form hydrogen gas.[46] Therefore, in this study, the adsorption of either cysteine molecules or pairs has been considered a hemolytic process.

Considering the computational effort and accuracy, we bonded as many as five cysteine molecules to the surface (five monolayer cysteine molecules and five bilayer pairs). It also needs to specifically explain herein the term "monolayer and bilayer" referred throughout the study. The pattern of either cysteine molecules or pairs anchoring on Au_{55} is considered a low coverage, compared to the practical experimental

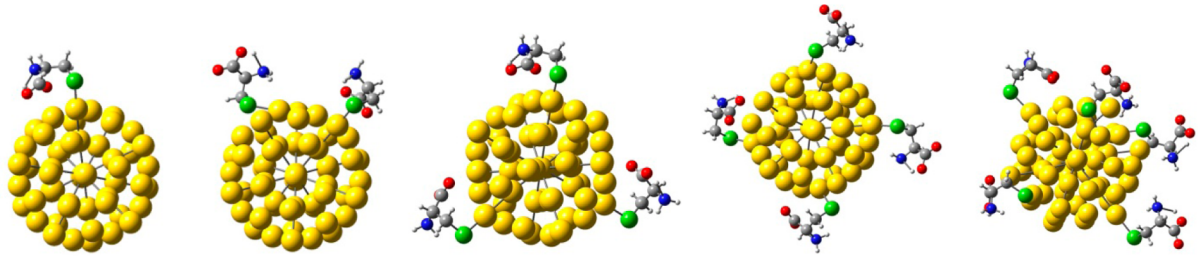

Figure 2. Monolayer structures of cysteine molecules on Au_{55}. Number of cysteine molecules is from 1 to 5. The yellow colored balls represent Au atoms. The green balls represent S atoms, and the gray balls are carbon atoms. The blue and red colored balls represent N and O atoms, respectively, and the white balls are the H atoms.

dx.doi.org/10.1021/jp308215n | J. Phys. Chem. C 2012, 116, 25816−25823

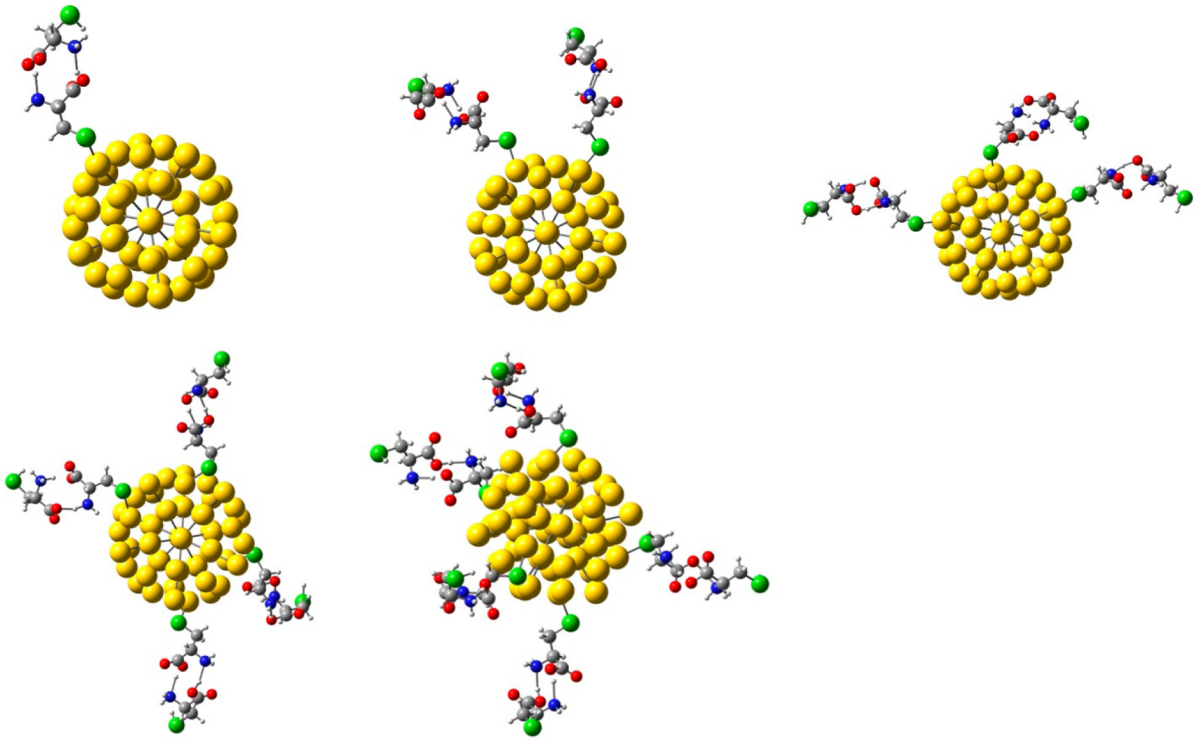

Figure 3. Bilayer structures of cysteine molecules on Au_{55}. Number of cysteine pairs is from 1 to 5 (2 to 10 cysteine molecules). The yellow colored balls represent Au atoms. The green balls represent S atoms, and the gray balls are carbon atoms. The blue and red colored balls represent N and O atoms, respectively, and the white balls are the H atoms.

concentration of L-cysteine.[25,47] Therefore, the terms of monolayer and bilayer used throughout imply the fractional layer for low cysteine coverage. Geometry optimizations produced stable structures for each configuration, meanwhile preserving the hydrogen bonds in the bilayer structures (see Figures 2 and 3). In the monolayer structures, the average Au−S bond length was 2.57 ± 0.46 Å, whereas in the bilayer structures, the bond length was 2.402 ± 0.045 Å on average. Notice that the bond length for monolayer structures is slightly longer than that of bilayer structures and has a magnitude larger variance. More importantly, the value for bilayer structures is consistent with the reported value of 2.39 Å,[48,49] leading us to propose that this might be the more preferable mode of the gold−cysteine system. Additionally, the average hydrogen bond length between layers of zwitterion cysteine in the bilayer structures was 1.49 ± 0.15 Å.

One way to compare whether the monolayer structure is favored over the bilayer structure (or vice versa) is to calculate the adsorption energies for each model, which we defined as

$$E_{ads} = E_{complex} - NE_{cysteine} - E_{Au55} + \frac{N}{2}E_{H2}$$

for monolayer configurations and

$$E_{ads} = E_{complex} - NE_{cysteine} - E_{Au55} + \frac{N}{4}E_{H2}$$

for bilayer structures, where $E_{complex}$ is the total energy of Au_{55} with adsorbates, $E_{cysteine}$ and E_{Au55} are the total energies of the cysteine molecule and isolated Au_{55} nanoparticle, respectively, and N is the numbers of cysteine molecules adsorbed on Au_{55}. The results of the adsorption energy calculation are listed in Table 2 (all the relevant information is listed in the Support Information) and are visually depicted in Figure 4. As shown in Figure 4, the magnitude of the adsorption energy increases in an approximately linear trend as the number of cysteine molecules increased, as would be expected. The bilayer structures appear to have lower adsorption energy overall than that of the monolayer structures, but showing more deviation from the linear trend. Particularly, for the four pairs and five pairs of cysteine appearing around Au_{55}, the adsorption energy tends to be close, which is possibly because of the limited surface area, which can accommodate higher density of anchoring cysteine. What is important, shown in Figure 4, is that there is a trend related to the total adsorption energy. Even though the starting point of bilayer model plot is higher than that of the monolayer model, the trend of the plots shows that

Table 2. Total Adsorption Energy with Respect to the Number of Cysteine Molecules Attached (for the Bilayer Model, the Average Adsorption Energy Is Defined As Per Cysteine Pair)

complex	total adsorption energy (eV)	average adsorption energy (eV)
Monolayer		
Au_{55} + 1cysteine	−1.155	−1.155
Au_{55} + 2cysteine	−2.976	−1.488
Au_{55} + 3cysteine	−3.125	−1.042
Au_{55} + 4cysteine	−6.250	−1.563
Au_{55} + 5cysteine	−8.899	−1.780
Bilayer		
Au_{55} + 2cysteine	−0.991	−0.991
Au_{55} + 4cysteine	−2.025	−1.013
Au_{55} + 6cysteine	−5.291	−1.764
Au_{55} + 8cysteine	−9.032	−2.258
Au_{55} + 10cysteine	−10.827	−2.165

dx.doi.org/10.1021/jp308215n | J. Phys. Chem. C 2012, 116, 25816−25823

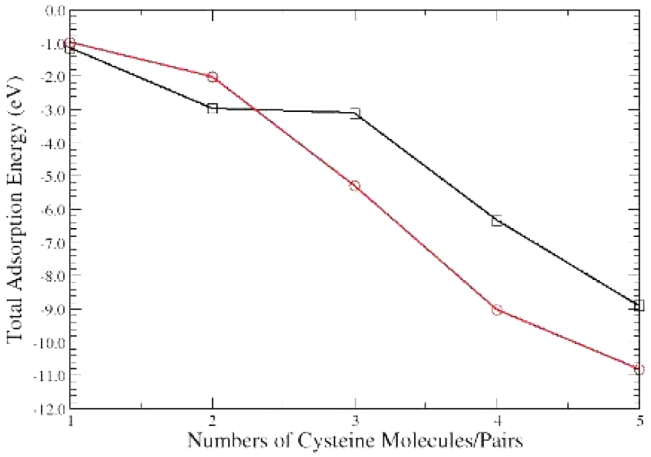

Figure 4. Total adsorption energy plots of monolayer and bilayer models. The black color plot corresponds to the five structures of the monolayer model; the red color plot corresponds to the five structures of the bilayer model.

the overall bilayer model tends to be more energetically preferable above the monolayer model. At this point, it will be meaningful to look into the electronic properties of all the structures calculated in this study.

3.2. Electronic Properties Analysis. Besides analyzing the geometric confirmations of the two models, we also analyze the electronic structures of each confirmation for both attaching modes. Since the primary focus of this study is to investigate how cysteine molecules interact with gold nanoparticles, in this case, Au_{55} nanocluster, we think one of the key factors in determining the attaching mode is to probe the charge transferring occurred between gold nanoparticles and cysteine molecules. Previous ^{1}H, ^{13}C, and ^{15}N MAS NMR experiments showed that there are two types of cysteine molecules presented in cysteine−gold nanoparticles systems. One type of cysteine was assigned to form an inner chemisorbed layer and the other type of cysteine formed an outer layer that interacts with the inner layer via hydrogen bonding. The ^{13}C chemical shift of the C_{α}, C_{β}, and C_{γ} carbons of the outer layer and the C_{α} carbon of the inner layer occurred at the same position as those observed or polycrystalline L-cysteine. Also, the observed ^{15}N chemical shift of the cysteine−gold nanoparticle system was only slightly shifted from the position observed for polycrystalline L-cysteine. However, the ^{13}C chemical shifts of the C_{α} and C_{β} carbons of the inner layer were deshielded by 12 ppm relative to the positions found in polycrystalline L-cysteine. Furthermore, a ^{1}H resonance was not observed at the expected position for a carboxyl proton, which indicates that the cysteine molecules appear as zwitterions. A ^{1}H resonance was observed for the −SH group, and its position was similar to that observed in polycrystalline cysteine and its intensity was consistent with the only half of all cysteine molecules contributing to the resonance (presumably the outer layer cysteine molecules)

In our calculations, we found the similar trend of the Mülliken charge distribution of each carbon atom in the bilayer structures. As shown in Table 3, we list the two sets of data of both monolayer and bilayer models. On the basis of the first set of the data, we find that the Mülliken charges of the three types of carbon atoms (C_{α}, C_{β}, and C_{γ}) all exhibit obvious differences from the initial values we obtained for isolated L-cysteine. The two carbon atoms (C_{β} and C_{γ}) closer to sulfur atoms tend to be more negative, while the C_{α} atoms obviously become more positive in charge density.

For the bilayer structure, the C_{α} and C_{α}' present minor charge differences in the gold−cysteine complex. This surprisingly small charge difference is possible for the reason that the cysteine pairs in bilayer model stabilize the H-bonding interactions present in solid L-cysteine. The outer layer cysteines will maintain interactions to the inner layer via H-bonding between charged amino and carboxyl groups. As a result, the C_{α} of each cysteine of the pair, exhibits almost the same value as the initial value of C_{α}. Even though the inner layer of cysteine is bonded to Au_{55} via the Au−S bond, apparently the changes in charge caused by the interaction between gold and the inner cysteine mostly appear on S, C_{β}, and C_{γ}. Therefore, we believe that the minor charge difference found in C_{α} of the bilayer model agrees with the minimal change in the ^{13}C chemical shift of the C_{α} carbon observed in the solid state NMR study. Even though we did not perform the chemical shift calculations in our study, the Mülliken charge

Table 3. Mülliken Atomic Charges (Given in the Units of *e*, the Elementary Charge) for the Three Carbon Atoms in Each Cysteine Molecule Attaching on A_{55}[a]

carbon	Mülliken charge				
monolayer	Au_{55}cysteine1	Au_{55}cysteine2	Au_{55}cysteine3	Au_{55}cysteine4	Au_{55}cysteine5
C_{α}	0.601(0.508)	0.554(0.508)	0.579(0.508)	0.528(0.508)	0.416(0.508)
C_{β}	−0.223 (−0.094)	−0.244 (−0.094)	−0.257 (−0.094)	−0.272 (−0.094)	−0.145 (−0.094)
C_{γ}	−0.628 (−0.241)	−0.635 (−0.241)	−0.655 (−0.241)	−0.661 (−0.241)	−0.534 (−0.241)
carbon	Mülliken charge				
bilayer	Au_{55}cysteine1B	Au_{55}cysteine2B	Au_{55}cysteine3B	Au_{55}cysteine4B	Au_{55}cysteine5B
C_{α}	0.521 (0.508)	0.519 (0.508)	0.517 (0.508)	0.513 (0.508)	0.527 (0.508)
C_{β}	−0.189 (−0.094)	−0.181 (−0.094)	−0.167 (−0.094)	−0.180 (−0.094)	−0.169 (−0.094)
C_{γ}	−0.632 (−0.241)	−0.638 (−0.241)	−0.627 (−0.241)	−0.650 (−0.241)	−0.652 (−0.241)
C_{α}'	0.519 (0.508)	0.520 (0.508)	0.517 (0.508)	0.520 (0.508)	0.525 (0.508)
C_{β}'	−0.191 (−0.094)	−0.192 (−0.094)	−0.174 (−0.094)	−0.173 (−0.094)	−0.171 (−0.094)
C_{γ}'	−0.620 (−0.241)	−0.620 (−0.241)	−0.617 (−0.241)	−0.610 (−0.241)	−0.609 (−0.241)

[a]Note that C_{α}, C_{β}, and C_{γ} correspond to the three carbon atoms in the cysteine of the inner layer and that C_{α}', C_{β}', and C_{γ}' correspond to the three carbon atoms in the cysteine of the outer layer. (The charge value is the average value of the same type of carbon atoms, except the structure Au_{55}cysteine1 and Au_{55}cysteine1B.) The Mülliken charge values shown in parentheses are the initial Mülliken charge values calculated for solid-state L-cysteine.

dx.doi.org/10.1021/jp308215n | J. Phys. Chem. C 2012, 116, 25816−25823

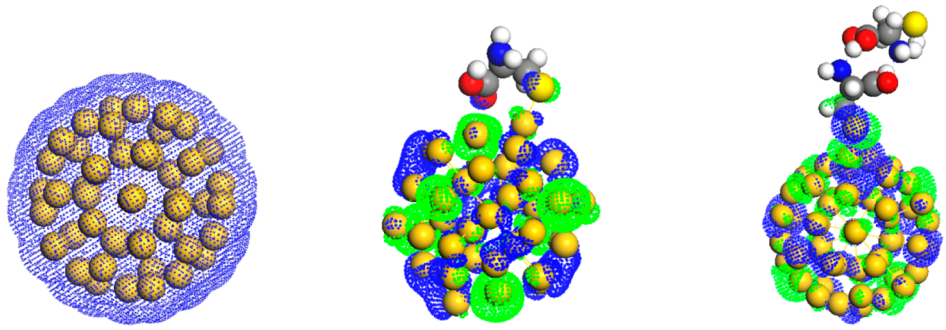

Figure 5. Charge density of Au_{55} nanoparticle and HOMO of Au_{55} with single cysteine molecule and single cysteine pair (the iso value is 0.015).

Table 4. Mülliken Atomic Charge (Given in the Units of *e*, the Elementary Charge) on the Sulfur Atoms of Monolayer and Bilayer Structures (the Charge Value Is the Average Value of the Sulfur Atoms, except the Structures Au55cysteine1 and Au55cysteine1B)

sulfur	Mülliken charge				
monolayer	Au_{55}cysteine1	Au_{55}cysteine2	Au_{55}cysteine3	Au_{55}cysteine4	Au_{55}cysteine5
S	−0.009 (−0.346)	0.004 (−0.346)	0.004 (−0.346)	0.135 (−0.346)	0.110 (−0.346)
sulfur	Mülliken charge				
bilayer	Au_{55}cysteine1B	Au_{55}cysteine2B	Au_{55}cysteine3B	Au_{55}cysteine4B	Au_{55}cysteine5B
S	0.280 (−0.346)	0.108 (−0.346)	0.120 (−0.346)	0.267 (−0.346)	0.244 (−0.346)
S′	−0.012 (−0.346)	−0.170 (−0.346)	−0.131 (−0.346)	−0.138 (−0.346)	−0.136 (−0.346)

distribution is one of the parameters to determine how the charge redistributes in the entire structure affected by the interaction between gold and cysteine. Our agreement with the NMR studies[14,25] confirms that the bilayer model we proposed in our calculations is more favorable than the monolayer model.

Further, we analyze the Mülliken charge of sulfur atoms in both monolayer and bilayer models. The bond nature of Au−S has been found to have covalent and electrostatic character.[50] For pure Au_{55} particle, the charge density (shown in Figure 5) is a negative charged shell wrapping a positive charged core, which is composed of the inner 13 Au atoms. With cysteine molecules anchoring to the Au_{55} surface, the charge distribution on both Au atoms and sulfur atoms exhibit charge shifts between Au and S atoms. In the monolayer structures, the sulfur atoms tend to be positively charged, except the single cysteine molecule attaching to the structure. Compared to the initial value −0.346 of S atom in L-cysteine, the sulfur atoms exhibit positive shifts in charge, listed in Table 4. The charges of sulfur atoms in the five monolayer structure become −0.009, 0.004, 0.004, 0.135, and 0.110, which are much more positive compared to the initial value (−0.346).

For the bilayer model, the sulfur atoms of the inner layer show remarkable charge shift from negative (−0.346) to positive values, as listed in Table 4. Compared to the charge shift of sulfur atoms in the monolayer cysteine structures, these sulfur atoms exhibit more positive charge shift, which supports our hypothesis that the interaction between Au and S atoms is much stronger. The sulfur atoms in the outer layer, however, still preserve negative charges, even the value is smaller compared to the initial value (−0.346). Even though the outer layer of cysteine is far from the Au_{55} particle, the charge distribution is still noticeable and results from the strong interaction between the inner layers and gold surface. In Figure 5, we show three diagrams of frontier orbitals (HOMO) for Au_{55}; Au_{55} with one cysteine molecule and one cysteine pair, respectively. As we can see, the obvious overlap between S and gold atoms demonstrates the strong interaction in Au−S. Therefore, we propose that the bilayer model is pronouncedly more favorable in the cysteine−gold particle complex. With the outer layer serving as a charge balancing shell, the inner layer is able to anchor to the gold particle via strong Au−S interaction.

There are still differences between the solid-state NMR experiments and our DFT calculations. For instance, two populations of cysteine signals were clearly observed. The size difference between the real sample (∼6 nm) and DFT calculation model (Au_{55} ≈ 1.4 nm) possibly accounts for certain unavoidable dissimilarity. We assume the large surface area in gold nanoparticle around 6 nm is possible to accommodate more cysteine pairs and maintains the H-bonding network horizontally, which might be the reason for the existence of two populations of cysteine signals. Limited by the computational cost, in this study, we considered the five cysteine molecules for monolayer and five cysteine pairs for bilayer. Higher cysteine coverage on gold nanoparticles certainly needs to be established for a more persuasive model. Therefore, a further study of a variety of cysteine coverage on gold nanoparticle is ongoing.

4. CONCLUSIONS

In this study, we investigated two possible attaching modes of L-cysteine molecules on the gold nanoparticle, Au_{55}. We found that cysteine bonds strongly to the gold nanoparticle via a strong Au−S interaction. Furthermore, cysteine can arrange in either a monolayer or bilayer configuration around the nanoparticle, which determines whether or not it has a zwitterion structure. In the bilayer model, the cysteine zwitterion structure is stabilized via the H-bonding between inner layer cysteine and outer layer cysteine. With the outer layer as a charge balance shell, the inner layer cysteine tends to anchor to the gold particle via a stronger interaction. The three

dx.doi.org/10.1021/jp308215n | J. Phys. Chem. C 2012, 116, 25816−25823

types of carbon atoms (C_α, C_β, and C_γ) of the inner and outer layers present the similar trend in terms of charge changes as what was observed in solid-state NMR spectrum. The two carbons (C_β and C_γ) closer to sulfur atoms exhibit higher charge changes, which correspond to the chemical shift signal detected, while for the C_α, the chemical shift preserves the original peak, which is similar to the minor charge changes shown in our calculations. Overall, we propose that the bilayer model is a possible arranging format for cysteine anchoring to gold nanoparticles, which enables the outer layer sulfur atoms to serve as an open portal for further biofunctional modification.

■ ASSOCIATED CONTENT

Supporting Information

Energy values of each component corresponding to Table 1. All relevant energetic values (total energy) corresponding to the 10 structures listed in Table 2. Coordinates of structures shown in Figures 2 and 3. This material is available free of charge via the Internet at http://pubs.acs.org.

■ AUTHOR INFORMATION

Corresponding Author

*E-mail: Hong.wang@mail.wvu.edu.

Notes

The authors declare no competing financial interest.

■ ACKNOWLEDGMENTS

This work is supported by Grant PRF51290-ND6 from the American Chemical Society Petroleum Research Fund. We also thank West Virginia University High Performance Computing Center for computational time, and the Gold Water Scholarship for supporting J.A.C. in the course of this work.

■ REFERENCES

(1) Cunningham, D. A. H.; et al. The Relationship between the Structure and Activity of Nanometer Size Gold When Supported on $Mg(OH)_2$. *J. Catal.* **1998**, *177* (1), 1−10.
(2) Mocanu, A.; et al. Self-Assembly Characteristics of Gold Nanoparticles in the Presence of Cysteine. *Colloids Surf., A* **2009**, *338* (1−3), 93−101.
(3) Daniel, M.-C.; Astruc, D. Gold Nanoparticles: Assembly, Supramolecular Chemistry, Quantum-Size-Related Properties, and Applications toward Biology, Catalysis, and Nanotechnology. *Chem. Rev.* **2003**, *104* (1), 293−346.
(4) Elder, R. C.; et al. EXAFS and WAXS Structure Determination for an Antiarthritic Drug, Sodium Gold(I) Thiomalate. *J. Am. Chem. Soc.* **1985**, *107* (17), 5024−5025.
(5) Love, J. C.; et al. Self-Assembled Monolayers of Thiolates on Metals as a Form of Nanotechnology. *Chem. Rev.* **2005**, *105* (4), 1103−1170.
(6) Mann, S.; et al. Biologically Programmed Nanoparticle Assembly. *Adv. Mater.* **2000**, *12* (2), 147−150.
(7) Chah, S.; Hammond, M. R.; Zare, R. N. Gold nanoparticles as a colorimetric sensor for protein conformational changes. *Chem. Biol.* **2005**, *12* (3), 323−328.
(8) Selvakannan, P. R.; et al. Water-Dispersible Tryptophan-Protected Gold Nanoparticles Prepared by the Spontaneous Reduction of Aqueous Chloroaurate Ions by the Amino Acid. *J. Colloid Interface Sci.* **2004**, *269* (1), 97−102.
(9) Bhargava, S. K.; et al. Gold Nanoparticle Formation during Bromoaurate Reduction by Amino Acids. *Langmuir* **2005**, *21* (13), 5949−5956.
(10) Aryal, S.; et al. Study of Electrolyte Induced Aggregation of Gold Nanoparticles Capped by Amino Acids. *J. Colloid Interface Sci.* **2006**, *299* (1), 191−197.
(11) Blankenburg, S.; Schmidt, W. G. Long-Range Chiral Recognition due to Substrate Locking and Substrate-Adsorbate Charge Transfer. *Phys. Rev. Lett.* **2007**, *99* (19), 196107.
(12) Zhang, J.; et al. Two-Dimensional Cysteine and Cystine Cluster Networks on Au(111) Disclosed by Voltammetry and in Situ Scanning Tunneling Microscopy. *Langmuir* **2000**, *16* (18), 7229−7237.
(13) Mandal, S.; Phadtare, S.; Sastry, M. Interfacing Biology with Nanoparticles. *Curr. Appl. Phys.* **2005**, *5* (2), 118−127.
(14) Abraham, A.; et al. Solid-State NMR Study of Cysteine on Gold Nanoparticles. *J. Phys. Chem. C* **2010**, *114* (42), 18109−18114.
(15) Gorbitz, C. H.; Dalhus, B. L-Cysteine, Monoclinic Form Redetermination at 120 K. *Acta Crystallogr., Sect. C: Cryst. Struct. Commun.* **1996**, *52* (7), 1756−1759.
(16) Jadzinsky, P. D.; et al. Structure of a Thiol Monolayer-Protected Gold Nanoparticle at 1.1 Angstrom Resolution. *Science* **2007**, *318* (5849), 430−433.
(17) Jiang, D. E.; et al. The "Staple" Motif: A Key to Stability of Thiolate-Protected Gold Nanoclusters. *J. Am. Chem. Soc.* **2008**, *130* (9), 2777−2779.
(18) Nishigaki, J.-I.; et al. A New Binding Motif of Sterically Demanding Thiolates on a Gold Cluster. *J. Am. Chem. Soc.* **2012**, *134* (35), 14295−14297.
(19) Krommenhoek, P. J.; et al. Bulky Adamantanethiolate and Cyclohexanethiolate Ligands Favor Smaller Gold Nanoparticles with Altered Discrete Sizes. *ACS Nano* **2012**, *6* (6), 4903−4911.
(20) Di Felice, R.; Selloni, A. Adsorption Modes of Cysteine on Au(111): Thiolate, Amino-Thiolate, Disulfide. *J. Chem. Phys.* **2004**, *120* (10), 4906−4914.
(21) Kuhnle, A.; et al. Chiral Recognition in Dimerization of Adsorbed Cysteine Observed by Scanning Tunnelling Microscopy. *Nature* **2002**, *415* (6874), 891−893.
(22) Höffling, B.; et al. Interface with Organic Molecules: Cysteine on Au(110). *Phys. Status Solidi C* **2010**, *7* (2), 149−152.
(23) Di Felice, R.; Selloni, A.; Molinari, E. DFT Study of Cysteine Adsorption on Au(111). *J. Phys. Chem. B* **2002**, *107* (5), 1151−1156.
(24) Häkkinen, H.; Barnett, R. N.; Landman, U. Electronic Structure of Passivated Au_{38}(SCH_{3})_{24} Nanocrystal. *Phys. Rev. Lett.* **1999**, *82* (16), 3264−3267.
(25) Abraham, A.; et al. H-1 MAS NMR Study of Cysteine-Coated Gold Nanoparticles. *J. Phys. Chem. B* **2012**, *116* (27), 7771−7775.
(26) Delley, B. From Molecules to Solids with the $Dmol^3$ Approach. *J. Chem. Phys.* **2000**, *113* (18), 7756−7764.
(27) Delley, B. An All-Electron Numerical Method for Solving the Local Density Functional for Polyatomic Molecules. *J. Chem. Phys.* **1990**, *92* (1), 508−517.
(28) Perdew, J. P.; Burke, K.; Ernzerhof, M. Generalized Gradient Approximation Made Simple. *Phys. Rev. Lett.* **1996**, *77* (18), 3865−3868.
(29) Grimme, S.; Ehrlich, S.; Goerigk, L. Effect of the Damping Function in Dispersion Corrected Density Functional Theory. *J. Comput. Chem.* **2011**, *32* (7), 1456−1465.
(30) Grimme, S.; et al. Consistent Theoretical Description of 1,3-Dipolar Cycloaddition Reactions. *J. Phys. Chem. A* **2006**, *110* (8), 2583−2586.
(31) Grimme, S.; Diedrich, C.; Korth, M. The Importance of Inter- and Intramolecular van der Waals Interactions in Organic Reactions: The Dimerization of Anthracene Revisited. *Angew. Chem., Int. Ed.* **2006**, *45* (4), 625−629.
(32) Grimme, S.; et al. A Consistent and Accurate ab Initio Parametrization of Density Functional Dispersion Correction (DFT-D) for the 94 Elements H-Pu. *J. Chem. Phys.* **2010**, *132* (15), 154104.
(33) Grimme, S. Seemingly Simple Stereoelectronic Effects in Alkane Isomers and the Implications for Kohn-Sham Density Functional Theory. *Angew. Chem., Int. Ed.* **2006**, *45* (27), 4460−4464.
(34) Luger, P.; Weber, M. DL-Cysteine at 298 K. *Acta Crystallogr., Sect. C: Cryst. Struct. Commun.* **1999**, *55* (11), 1882−1885.

(35) Chapman, R. P.; Bryce, D. L. A High-Field Solid-State 35/37Cl NMR and Quantum Chemical Investigation of the Chlorine Quadrupolar and Chemical Shift Tensors in Amino Acid Hydrochlorides. *Phys. Chem. Chem. Phys.* **2007**, *9* (47), 6219−6230.
(36) Ritchie, S. M. C.; et al. Polycysteine and Other Polyamino Acid Functionalized Microfiltration Membranes for Heavy Metal Capture. *Environ. Sci. Technol.* **2001**, *35* (15), 3252−3258.
(37) Liu, A.-C.; et al. Application of Cysteine Monolayers for Electrochemical Determination of Sub-ppb Copper(II). *Anal. Chem.* **1999**, *71* (8), 1549−1552.
(38) Uvdal, K.; Bodö, P.; Liedberg, B. L-Cysteine Adsorbed on Gold and Copper: An X-ray Photoelectron Spectroscopy Study. *J. Colloid Interface Sci.* **1992**, *149* (1), 162−173.
(39) Vogel, W.; Rosner, B.; Tesche, B. Structural Investigations of Gold (Au55) Organometallic Complexes by X-ray Powder Diffraction and Transmission Electron Microscopy. *J. Phys. Chem.* **1993**, *97* (45), 11611−11616.
(40) Schmid, G.; et al. Naked Au55 Clusters: Dramatic Effect of a Thiol-Terminated Dendrimer. *Chem.—Eur. J.* **2000**, *6* (9), 1693−1697.
(41) Pei, Y.; et al. Investigating Active Site of Gold Nanoparticle Au55(PPh3)12Cl6 in Selective Oxidation. *ACS Nano* **2010**, *4* (4), 2009−2020.
(42) Schmid, G. The Relevance of Shape and Size of Au-55 Clusters. *Chem. Soc. Rev.* **2008**, *37* (9), 1909−1930.
(43) Chang, C. M.; Cheng, C.; Wei, C. M. CO Oxidation on Unsupported Au_{55}, Ag_{55}, and $Au_{25}Ag_{30}$ Nanoclusters. *J. Chem. Phys.* **2008**, *128* (12), 124710−4.
(44) Chen, F.; et al. Effect of Anchoring Groups on Single-Molecule Conductance: Comparative Study of Thiol-, Amine-, and Carboxylic-Acid-Terminated Molecules. *J. Am. Chem. Soc.* **2006**, *128* (49), 15874−15881.
(45) Cohen-Atiya, M.; Mandler, D. Studying Thiol Adsorption on Au, Ag and Hg Surfaces by Potentiometric Measurements. *J. Electroanal. Chem.* **2003**, *550*−*551* (0), 267−276.
(46) Matthiesen, J. E.; et al. Loss of Hydrogen upon Exposure of Thiol to Gold Clusters at Low Temperature. *J. Am. Chem. Soc.* **2012**, *134* (22), 9376−9379.
(47) Johnson, E. R.; Becke, A.D. A post-Hartree-Fock model of intermolecular interactions: Inclusion of higher-order corrections. *J. Chem. Phys.* **2006**, *124* (17), 174104.
(48) Kaun, C.-C.; Guo, H. Resistance of Alkanethiol Molecular Wires. *Nano Lett.* **2003**, *3* (11), 1521−1525.
(49) Yin, X.; et al. Theoretical Analysis of Geometry-Correlated Conductivity of Molecular Wire. *Chem. Phys. Lett.* **2006**, *422* (1−3), 111−116.
(50) Pakiari, A. H.; Jamshidi, Z. Nature and Strength of M−S; Bonds (M = Au, Ag, and Cu) in Binary Alloy Gold Clusters. *J. Phys. Chem. A* **2010**, *114* (34), 9212−9221.